Direct Extraction of Equivalent Circuit Parameters for Heterojunction Bipolar Transistors

Ce-Jun Wei, *Member, IEEE,* and James C. M. Hwang, *Fellow, IEEE*

Abstract—**A new method is presented for the direct extraction of hybrid-T equivalent circuits for heterojunction bipolar transistors. The method differs from previous ones by extracting the equivalent circuit without using test structures or numerical optimization techniques. Instead, all equivalent circuit parameters are calculated analytically from small-signal S-parameters measured under different bias conditions. The analysis includes the distributed nature of the HBT base. The calculated parameters are essentially frequency-independent and they exhibit systematic bias dependence over the typical operating range of the transistor. Thus, the present method ensures unique and physically meaningful parameters for transistor design improvement and large-signal circuit simulation. In addition, the present method is much faster than the numerical optimization method.**

I. Introduction

TO DETERMINE a transistor's equivalent circuit parameters, the direct extraction method is superior to the numerical optimization method, especially in terms of efficiency and uniqueness. However, direct extraction has been difficult for the heterojunction bipolar transistor (HBT) due to the distributed nature of its base electrode. As listed in Table I, most of previously reported extraction methods rely on either special test structures [1] or numerical optimization techniques [2]–[5] to various degrees. For example, the method of [2] is largely analytical with only the emitter parameters extracted numerically. However, it omits the distributed base effect hence can result in non-physical parameter values such as negative collector resistances. In [6], we reported, for the first time, a direct extraction method which depends on neither test structures nor optimization techniques. The extraction is based on a hybrid-T equivalent circuit (Fig. 1) which resembles the HBT physical structure and, therefore, allows insights for device design improvement. We shall expand on [6] by deriving the equations in steps and describing the refined parameter extraction procedure in detail.

Briefly, the present procedure is based solely on the HBT S-parameters measured at different frequencies and biases. First, the extrinsic parasitic impedances associated with the base, emitter and collector are extracted from the S-parameters at the offset (open-collector) bias. Second, the ratio of internal vs. external base-collector capacitance is determined from the high-frequency S-parameters under forward-active biases. Finally, the intrinsic HBT parameters are calculated from the S-parameters at all frequencies and biases.

Manuscript received June 15, 1994; revised May 25, 1995. This work was supported in part by the Air Force Office of Scientific Research Grant 90-0302.

The authors are with Lehigh University, Bethlehem PA 18015 USA.

IEEE Log Number 9413426.

TABLE I
HBT Equivalent Circuit Extraction Methods

Equivalent Circuit	Parasitic De-embedding	Parameter Optimization	Reference
hybrid II	test structure, open collector	none	[1]
simplified T	low f approx.	R_{BE}, C_{BE}, R_E, L_E	[2]
simplified T	low f approx.	R_B/R_{B2}, C_{BC}, C_{BE}, C_{CE}	[3]
hybrid II	low f approx.	R_B, R_{B2}, C_{BE}, C_C	[4]
hybrid T	low f approx., cold HBT	R_B/R_{B2}, R_{CE}, C_{CE}, C_B	[5]
hybrid T	open collector, low/high f approx.	none	[6]

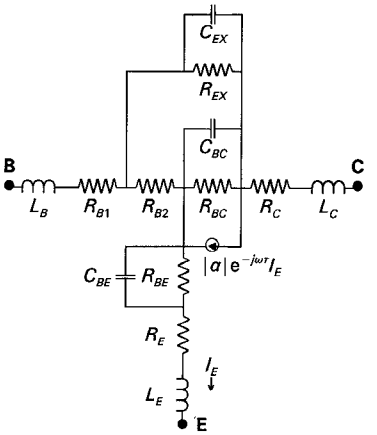

Fig. 1. Hybrid-T equivalent circuit reflecting the distributed nature of the HBT base.

II. Theory

A. Equivalent Circuit Modeling

The hybrid-T equivalent circuit used in the present method consists of several block impedances as shown in Fig. 1. The distributed base is represented by a combination of internal base-collector impedance Z_{BC}, external base-collector impedance Z_{EX}, intrinsic base resistance R_{B2}, and extrinsic base impedance Z_B. The base-emitter junction impedance is represented by Z_{BE}. The extrinsic collector and emitter impedances are denoted by Z_C and Z_E, respectively. Z_{BC}, Z_{EX},

and Z_{BE} each consists of a resistor and a capacitor in parallel, namely, $R_{BC}\|C_{BC}, R_{EX}\|C_{EX}$ and $R_{BE}\|C_{BE}$. Z_B, Z_C, and Z_E each consists of a resistor and an inductor in series, namely, R_B-L_B, R_C-L_C, and R_E-L_E. The base transport factor α is expressed in terms of a current gain $|\alpha|$ and a delay time τ. $\alpha = |\alpha|\exp(-j\omega\tau)$, where ω is the angular frequency. The extrinsic pad capacitances are not included because they have little impact on the HBT performance over the frequencies of interest and the S-parameters are measured on-wafer.

Thus, the equivalent circuit contains nine intrinsic and six extrinsic parameters. The six extrinsic parameters, namely, R_B, R_C, R_E, L_B, L_C, and L_E, are assumed to be independent of bias or frequency hence can be extracted from low- and high-frequency S-parameters measured with the HBT under offset biases. The nine intrinsic parameters can be reduced to eight unknowns if the ratio $\gamma = C_{EX}/(C_{BC}+C_{EX})$ is known. This ratio can be estimated from the HBT geometry, knowing the base width, emitter width, and base-emitter spacing. Or, in the present case, is determined by the high-frequency S-parameters at a forward-active bias. Once γ is known, all intrinsic parameters can be solved exactly at each frequency from the real and imaginary parts of the four S-parameters measured with the HBT under normal biases.

The open-circuit z-parameters of the equivalent circuit of Fig. 1 can be expressed as in the following

$$z_{11} = \frac{[(1-\alpha)Z_{BC} + Z_{EX}]R_{B2}}{Z_{BC} + Z_{EX} + R_{B2}} + Z_{BE} + Z_B + Z_E \quad (1)$$

$$z_{12} = \frac{(1-\alpha)Z_{BC}R_{B2}}{Z_{BC} + Z_{EX} + R_{B2}} + Z_{BE} + Z_E \quad (2)$$

$$z_{21} = \frac{[-\alpha Z_{EX} + (1-\alpha)R_{B2}]Z_{BC}}{Z_{BC} + Z_{EX} + R_{B2}} + Z_{BE} + Z_E \quad (3)$$

$$z_{22} = \frac{(1-\alpha)Z_{BC}(Z_{EX} + R_{B2})}{Z_{BC} + Z_{EX} + R_{B2}} + Z_{BE} + Z_C + Z_E. \quad (4)$$

Therefore

$$\frac{Z_{EX}R_{B2}}{Z_{BC} + Z_{EX} + R_{B2}} + Z_B = z_{11} - z_{12} \quad (5)$$

$$\frac{(1-\alpha)Z_{BC}R_{B2}}{Z_{BC} + Z_{EX} + R_{B2}} + Z_{BE} + Z_E = z_{12} \quad (6)$$

$$\frac{\alpha Z_{BC}Z_{EX}}{Z_{BC} + Z_{EX} + R_{B2}} = z_{12} - z_{21} \quad (7)$$

$$\frac{Z_{BC}Z_{EX}}{Z_{BC} + Z_{EX} + R_{B2}} + Z_C = z_{22} - z_{21}. \quad (8)$$

The above expressions will reduce to that of [2] if the distributed nature of the base can be neglected, i.e., $R_{B2} \approx 0$ and Z_{BC} and Z_{EX} are lumped together. However, this is usually not valid for HBTs, even at the low-frequency limit with $R_{B2} \ll R_{BC}$ and $R_{B2} \ll R_{EX}$. Notice that, in this case, the first terms of (5) and (6) will reduce to a fixed fraction of R_{B2}, depending on how the total base-collector impedance is distributed among R_{BC} and R_{EX}. If the impedance is distributed among a large number of elements, these terms will approach the familiar form of $R_{B2}/3$ for a transmission line. Presently, we believe the distribution among two elements is a reasonable compromise between physical resemblance, accuracy, and efficiency. At the high-frequency limit, the first terms of (7) and (8) will have a real contribution proportional to $-1/\omega^2 R_{B2}C_{BC}C_{EX}$. If this R_{B2} contribution is not accounted for in the extraction procedure, R_C may never approach a constant value and may even turn negative.

B. Extraction of Extrinsic Parameters

The extrinsic parasitic elements Z_B, Z_C, and Z_E are first determined from the S-parameters measured at the offset bias point, or the so-called "open-collector" condition [7], where both the base-collector and base-emitter junctions are in such forward conduction that the collector current is canceled out. With the junction forward-biased, $R_{B2} \gg R_{BC}$ and $R_{B2} \gg R_{EX}$. If the frequency is also low, C_{BC}, C_{EX}, and C_{BE} can be neglected. Therefore, from (5), (6), and (8)

$$\begin{aligned}\frac{R_{EX}R_{B2}}{R_{BC} + R_{EX} + R_{B2}} + R_B &\approx R_{EX} + R_B \\ &\approx \frac{n_{EX}V_T}{I_{EX}} + R_B \\ &\approx \text{Real}\,(z_{11} - z_{12}) \end{aligned} \quad (9)$$

$$\begin{aligned}\frac{(1-\alpha_0)R_{BC}R_{B2}}{R_{BC} + R_{EX} + R_{B2}} + R_{BE} + R_E &\approx (1-\alpha_0)R_{BC} + R_{BE} + R_E \\ &\approx (1-\alpha_0)\frac{n_{BC}V_T}{I_{BC}} + \frac{n_{BE}V_T}{I_B} + R_E \\ &\approx \text{Real}\, z_{12} \end{aligned} \quad (10)$$

$$\frac{R_{BC}R_{EX}}{R_{BC} + R_{EX} + R_{B2}} + R_C \approx R_C \approx \text{Real}\,(z_{22} - z_{21}) \quad (11)$$

where α_0 is the common-base dc current gain; V_T is the thermal voltage; n_{BC}, n_{EX}, and n_{BE} are the ideality factors for the internal base-collector, external base-collector, and base-emitter junctions, respectively; I_{BC} and I_{EX} are the currents flowing through the internal and external base-collector junctions, respectively; I_B is the total base current. Notice that $I_{BC} + I_{EX} = \alpha_0 I_B$ under the open-collector condition. Since the ratio of I_{BC} versus I_{EX} is approximately constant, these dc currents will all increase with increasing base injection and the left sides of (9)–(11) will approach R_B, R_E, and R_C, respectively. Therefore, the extrinsic resistances can be obtained by plotting the real parts of low-frequency $z_{11} - z_{12}, z_{12}$, and $z_{22} - z_{21}$ as functions of the inverse base current and extrapolating for their intercepts with $I_B = \infty$. The extrinsic inductances L_B, L_E, and L_C are similarly obtained from the imaginary parts of $z_{11} - z_{12}, z_{12}$, and $z_{22} - z_{21}$ at high frequencies.

C. Extraction of Intrinsic Parameters

With the extrinsic parasitic impedances determined, we next focus on the parameters associated with the distributed base. The four (counting real and imaginary parts separately)

equations of (5) and (8) contain five unknowns, namely $R_{BC}, C_{BC}, R_{EX}, C_{EX}$, and R_{B2}. To solve for them, an additional condition is required. This requirement is satisfied by finding the ratio $\gamma = C_{EX}/(C_{BC}+C_{EX})$ which is mainly determined by geometry hence independent of frequency. For HBTs with high Early voltage and high operating frequency, Z_{BC} and Z_{EX} are dominated by C_{BC} and C_{EX}. Therefore, from (5) and (8)

$$\frac{\frac{R_{B2}}{\omega C_{EX}}\left(\frac{1}{\omega C_{BC}}+\frac{1}{\omega C_{EX}}-jR_{B2}\right)}{\left(\frac{1}{\omega C_{BC}}+\frac{1}{\omega C_{EX}}\right)^2+R_{B2}^2} \approx z_{11}-z_{12}-Z_B \tag{12}$$

$$-\frac{\frac{1}{\omega^2 C_{BC}C_{EX}}\left[R_{B2}+j\left(\frac{1}{\omega C_{BC}}+\frac{1}{\omega C_{EX}}\right)\right]}{\left(\frac{1}{\omega C_{BC}}+\frac{1}{\omega C_{EX}}\right)^2+R_{B2}^2} \approx z_{22}-z_{21}-Z_C. \tag{13}$$

Dividing between the real parts of (12) and (13)

$$\gamma = \frac{C_{EX}}{C_{BC}+C_{EX}} \approx -\frac{\text{Real}\,(z_{22}-z_{21}-Z_C)}{\text{Real}\,(z_{11}-z_{12}-Z_B)}. \tag{14}$$

Thus, γ can be readily calculated and all the intrinsic HBT parameters can in turn be evaluated.

Dividing (8) directly by (5)

$$\frac{Z_{BC}}{R_{B2}} = \frac{z_{22}-z_{21}-Z_C}{z_{11}-z_{12}-Z_B}. \tag{15}$$

Therefore

$$\frac{R_{BC}}{R_{B2}} = \text{Real}\left(\frac{z_{22}-z_{21}-Z_C}{z_{11}-z_{12}-Z_B}\right) \tag{16}$$

$$\delta = R_{B2}\omega C_{BC} = -\frac{1}{\text{Imag}\left(\frac{z_{22}-z_{21}-Z_C}{z_{11}-z_{12}-Z_B}\right)} \tag{17}$$

where δ is defined for the sake of convenience. Substituting γ and δ in the imaginary part of (13), we have

$$C_{EX} = \frac{1}{\omega\gamma\left(\frac{1}{\gamma^2}+\delta^2\right)\text{Imag}(Z_C+z_{21}-z_{22})}. \tag{18}$$

Since all the quantities on the right side of (18) are known, C_{EX} is readily evaluated. Knowing C_{EX}, C_{BC} can be calculated from (14). Knowing C_{BC}, R_{B2} can in turn be calculated from (17). Next, R_{BC} is evaluated by using (16) and R_{EX} by using (5). For the typical HBT operation under a reverse base-collector bias, R_{BC} and R_{EX} are relatively large and difficult to determine precisely. It may be necessary to fix R_{BC} and R_{EX} at the low-frequency limit or average across the band. As they have relatively small impact on the HBT performance, they do not have to be determined precisely.

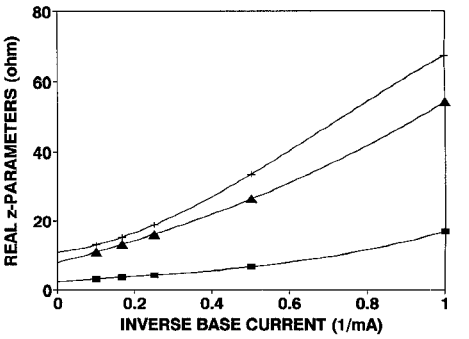

Fig. 2. Extraction of base, collector and emitter resistances, R_B, R_C, and R_E, from intercepts of (■) Real$(z_{11}-z_{12})$, (+) Real$(z_{22}-z_{21})$ and (▲) Real(z_{12}), respectively, with the vertical axis. $I_C = 0 \cdot f = 1$ GHz.

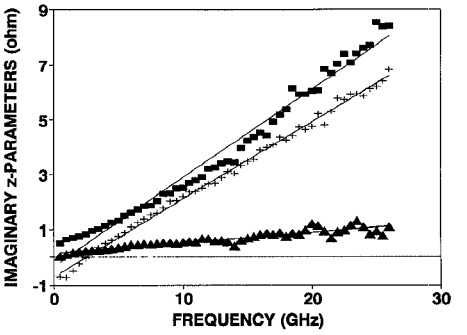

Fig. 3. Extraction of base, collector and emitter inductances, L_B, L_C, and L_E, from frequency dependence of (■) Imag$(z_{11}-z_{12})$, (+) Imag$(z_{22}-z_{21})$ and (▲) Imag(z_{12}). $I_C = 0 \cdot I_B = 10$ mA.

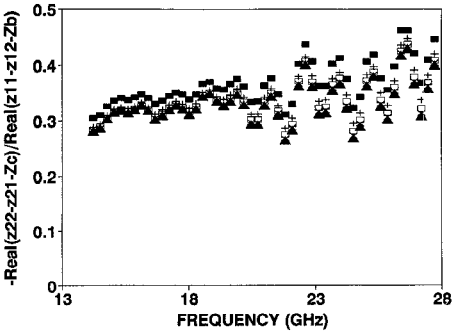

Fig. 4. Determination of external fraction of base-collector capacitance γ from the ratio of real z-parameters at high frequencies. $V_{CE} = 2$ V $\cdot$ $I_C =$ (■)3, (+)5, (□)7, (×)9, and (▲) 11 mA.

At this point, the remaining unknowns are α and Z_{BE} which can be solved by using (7) and (6), respectively. Dividing (7) by (8)

$$|\alpha|e^{-j\omega\tau} = \frac{z_{12}-z_{21}}{z_{22}-z_{21}-Z_C}. \tag{19}$$

Hence, α and τ can be evaluated from the magnitude and phase of the right side of (19). With α known, R_{BE} and C_{BE} can be evaluated from the real and imaginary parts of (6) after rearrangement

$$Z_{BE} = z_{12} - Z_E - \frac{(1-\alpha)Z_{BC}R_{B2}}{Z_{BC}+Z_{EX}+R_{B2}}. \tag{20}$$

Thus all the equivalent circuit parameters are derived.

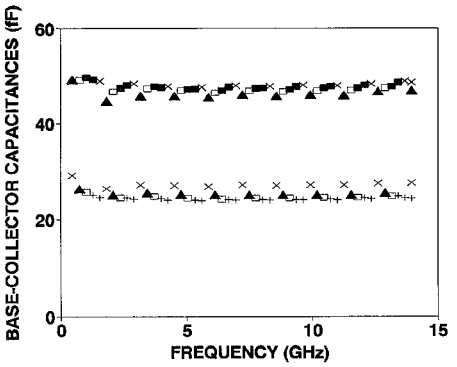

Fig. 5. Extracted internal and external base-collector capacitances, (top) C_{BC} and (bottom) C_{EX}. $V_{CE} = 2$ V $\cdot$ $I_C = (\blacksquare)3, (+)5, (\square)7, (\times)9$, and $(\blacktriangle)$ 11 mA.

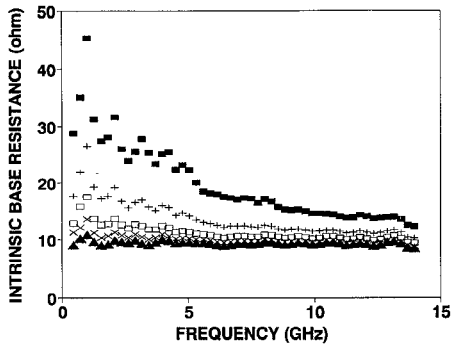

Fig. 6. Extracted intrinsic base resistance R_{B2}. $V_{CE} = 2$ V $\cdot$ $I_C = (\blacksquare)3$, $(+)5, (\square)7, (\times)9$, and $(\blacktriangle)$ 11 mA.

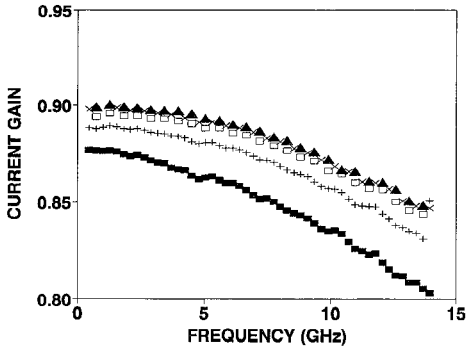

Fig. 7. Extracted current gain $|\alpha|$ of the base transport factor. $V_{CE} = 2$ V $\cdot$ $I_C = (\blacksquare)3, (+)5, (\square)7, (\times)9$, and $(\blacktriangle)$ 11 mA.

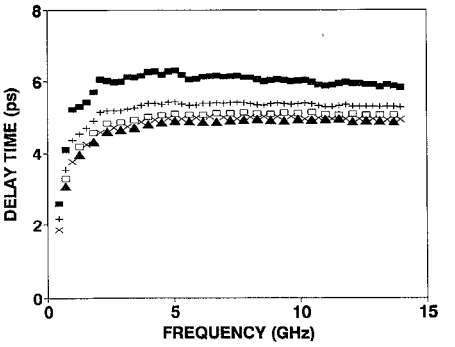

Fig. 8. Extracted delay time τ of the base transport factor. $V_{CE} = 2$ V $\cdot$ $I_C = (\blacksquare)3, (+)5, (\square)7, (\times)9$, and $(\blacktriangle)$ 11 mA.

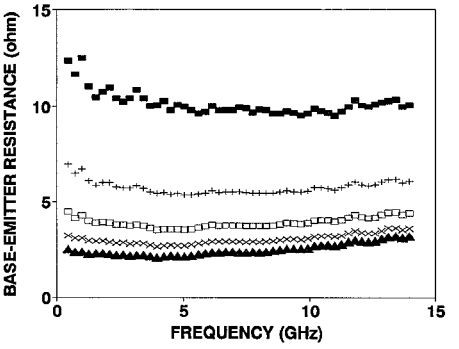

Fig. 9. Extracted base-emitter resistance R_{BE}. $V_{CE} = 2$ V $\cdot$ $I_C = (\blacksquare)3$, $(+)5, (\square)7, (\times)9$, and $(\blacktriangle)$ 11 mA.

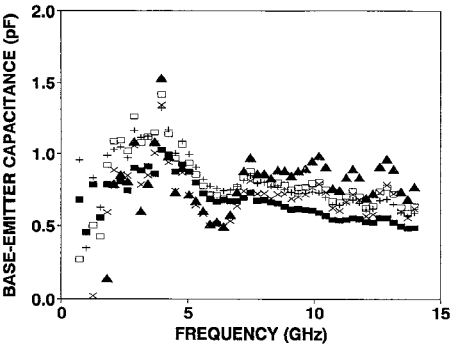

Fig. 10. Extracted base-emitter capacitance C_{BE}. $V_{CE} = 2$ V $\cdot$ $I_C = (\blacksquare)3, (+)5, (\square)7, (\times)9$, and $(\blacktriangle)$ 11 mA.

III. Results and Discussion

To illustrate the above method, we present the extracted equivalent circuit parameters for an N-p-n AlGaAs/GaAs HBT. The HBT contains three emitters, each emitter being 2 μm wide and 8 μm long. Typically, the HBT is biased in the common-emitter forward-active region with the collector-emitter voltage $V_{CE} = 2$ V and the collector current $I_C = 3$–11 mA. S-parameters were measured on-wafer from 0.2–27.2 GHz then converted to z-parameters. The current and power gain cut-off frequencies are in the 25–30 GHz range.

At first, the HBT was biased at the offset points ($V_{CE} \approx 0.3$ V; $I_C = 0$) for extraction of the extrinsic parasitic parameters. Fig. 2 shows that, at 1 GHz, the intercepts of the real parts of $z_{11} - z_{12}, z_{12}$, and $z_{22} - z_{21}$ with the vertical axis correspond to: $R_B = 3.3\ \Omega, R_C = 10\ \Omega$, and $R_E = 7.4\ \Omega$. Similarly, as shown in Fig. 3, the high-frequency slopes of the imaginary parts of $z_{11} - z_{12}, z_{12}$, and $z_{22} - z_{21}$ yield: $L_B = 0.050$ nH, $L_C = 0.044$ nH, and $L_E = 0.008$ pH.

Next, the HBT is forward-active biased and the high-frequency S-parameters used to determine the external base-collector capacitance ratio γ. Fig. 4 shows that the ratio of $\mathrm{Real}(z_{22} - z_{21} - Z_C)$ versus $\mathrm{Real}(z_{11} - z_{12} - Z_B)$ is bias-

TABLE II
TYPICAL HBT EQUIVALENT CIRCUIT PARAMETERS $V_{CE} = 2$ V; $I_C = 9$ mA

Parameter	Value	Parameter	Value
C_{BC}	0.047 pF	R_{B2}	10 Ω
C_{EX}	0.026 pF	R_B	2.3 Ω
C_{BE}	0.78 pF	R_C	11 Ω
R_{BC}	18 kΩ	R_E	7.8 Ω
R_{EX}	28 kΩ	L_B	0.051 nH
R_{BE}	3.3 Ω	L_C	0.045 nH
α_0	0.90	L_E	0.006 nH
τ	4.9 ps		

independent and it gradually approaches a constant value of γ =0.4 at high frequencies.

This constant γ was used to calculate all the intrinsic parameters. Fig. 5 shows that the resulted base-collector capacitances C_{BC} and C_{EX} are well behaved independent of frequency or bias. On the other hand, as shown in Fig. 6, the intrinsic base resistance R_{B2} varies with both frequency and bias, confirming that the distributed nature of the base cannot be ignored. Fig. 7 shows that, as expected, the current gain $|\alpha|$ increases with the injection level but decreases with frequency. Meanwhile, the delay time τ decreases with the injection level but is relatively independent of frequency above 2 GHz (Fig. 8). The extracted base-emitter impedance also exhibits the expected behavior. Figs. 9 and 10 show that R_{BE} decreases with current while C_{BE} increases with current. They are both relatively independent of frequency except that C_{BE} fluctuates significantly with frequency due to uncertainty in the extracted parasitic inductances. The above results demonstrate that, with proper account of the frequency-dependent nature of the distributed base, the extracted parameters are mostly frequency-independent so that the intrinsic HBT transport mechanism is reflected in the current gain factor. On the other hand, both the current gain factor and base-emitter impedance exhibit strong bias dependence and are the major sources of HBT non-linearity.

The above extracted parameters are summarized in Table II for a typical bias condition with V_{CE} =2 V and I_C =9 mA. These parameters were used to simulate the four S-parameters based on the equivalent circuit of Fig. 1. Fig. 11 shows that the simulated S-parameters are in good agreement with the measured ones from 1–20 GHz except the kink in S_{22} measured at high frequencies. When similar comparisons were made over all biases and frequencies, the worst case average error was 0.06 which is at least partially attributable to the measurement uncertainty at low currents.

IV. CONCLUSION

For the first time, all the equivalent circuit parameters of an HBT were directly extracted from S-parameters, without using test structures or optimization techniques. In addition to efficient computation, unique and accurate solutions, this new method resulted in frequency-independent parameters that vary systematically with bias. Consequently, these parameters are very valuable for device design improvement and large-signal circuit simulation.

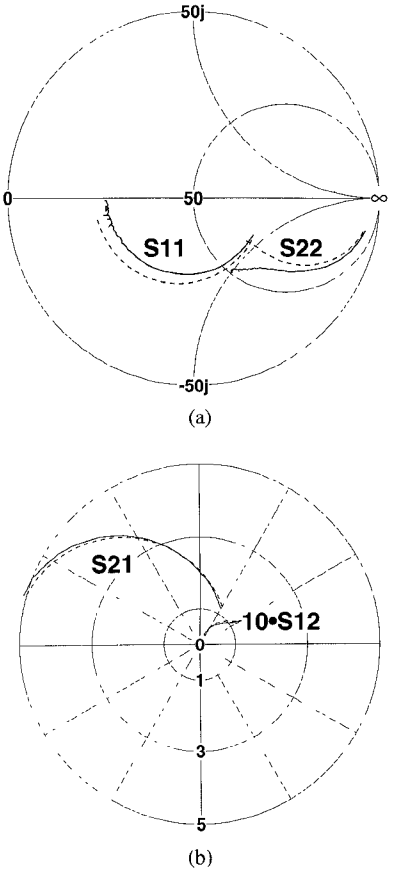

Fig. 11. Comparison of (—) simulated versus (×) measured S-parameters from 1–20 GHz. $V_{CE} = 2$ V · $I_C = 9$ mA.

ACKNOWLEDGMENT

The authors wish to thank the Air Force Wright Laboratory, particularly G. J. Trombley, M. E. Cheney, and C. I. Huang, for supplying transistors.

REFERENCES

[1] D. Costa, W U. Liu, and J. S. Harris, "Direct extraction of the AlGaAs/GaAs heterojunction bipolar transistor small-signal equivalent circuit," *IEEE Trans. Electron Devices*, vol. 38, pp. 2018–2024, Sept. 1991.

[2] D. R. Pehlke and D. Pavlidis, "Direct calculation of the HBT equivalent circuit form measured S-parameters," in *IEEE MTT-S Int. Microwave Symp. Dig.*, 1992, pp. 735–738.

[3] S. A. Maas and D. Tait, "Parameter-extraction method for heterojunction bipolar transistors," *IEEE Microwave and Guided Wave Lett.*, vol. 2, pp. 502–504, Dec. 1992.

[4] D. Wu and D. L. Miller, "Unique determination of AlGaAs/GaAs HBT's small-signal equivalent circuit parameters," in *Tech. Dig. IEEE GaAs IC Symp.*, 1993, pp. 259–262.

[5] L. M. Cacho, A. Werthof, and G. Kompa, "Broadband 40 GHz Si/SiGe HBT equivalent circuit using a successive analytical model parameter extraction," in *Dig. European Microwave Conf.*, 1993, pp. 515–517.

[6] C. J. Wei and J. C. M. Hwang, "New method for direct extraction of HBT equivalent circuit parameters," in *IEEE MTT-S Int. Microwave Symp. Dig.*, 1994, pp. 1245–1248.

[7] L. J. Ciacoletto, "Measurement of emitter and collector series resistances," *IEEE Trans. Electron Devices*, vol. ED-19, pp. 692–693, May 1972.

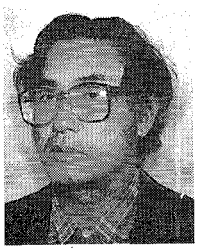

Ce-Jun Wei (M'93) received the B.S. degree from Qinghua University, China, in 1962, and the Ph.D. degree from the Chinese Academy of Sciences in 1966, both in electrical engineering.

He is currently a Senior Research Scientist at the Compound Semiconductor Technology Laboratory, Lehigh University. From 1966 to 1989, he worked on the modeling and characterization of microwave devices and circuits at the Semiconductor Institute of Chinese Academy of Sciences. Between 1980 and 1982, he worked on opto-electronics as a Visiting Professor at the Technical Institute of Aachen in Germany. He then returned to work on heterojunction devices in the Chinese Academy of Sciences and was promoted to Full Professor. From 1986 to 1988, he was a Visiting Scientist at Heinrich-Hertz-Institute and the Institute of solid-state physics in Berlin Technical University, working on opto-electronic devices. He joined Lehigh University in 1989. He has published more than 40 technical papers.

James C. M. Hwang (M'77–SM'82–F'94) received the B.S. degree in physics from the National Taiwan University in 1970. He received the M.S. and Ph.D. degrees in materials science and engineering from Cornell University in 1973 and 1976, respectively.

He is currently Professor of Electrical Engineering and Director of Compound Semiconductor Technology Laboratory, Lehigh University. Prior to joining Lehigh in 1988, he had 12 years of industrial experience working at IBM, AT&T, GE, and Gain Electronics. He has been a Consultant for the Air Force Wright Laboratory and the Aerospace Corp., in the area of microwave devices and integrated circuits. He has also been a director of Quantum Epitaxial Designs, a GaAs epitaxial wafer supplier which he helped found at Lehigh University's small-business incubation facility.